 DOI 10.1515/aot-2013-0028 — Adv. Opt. Techn. 2013; 2(4): 301–311

Review Article

Rolf Wester* and Axel Bäuerle

Light shaping for illumination

Abstract: The ever-increasing use of LED as a solid-state light source in general and specialized lighting has pushed the field of optics further for illumination towards sophistication and high precision. In this paper, we provide an overview of this domain, starting with a formulation of the underlying, fundamental mathematical problem, which in itself is not easily and directly solvable. We then describe various algorithms that have been developed as approximations for specialized cases, providing references to the relevant publications. Finally, two examples show the new possibilities in light shaping that have been made possible through the use of nonimaging freeform optics.

Keywords: extended source; illumination design; nonimaging optics; point source.

OCIS codes: 220.2945; 220.4298.

***Corresponding author: Rolf Wester,** Fraunhofer Institute for Laser Technology ILT, Steinbachstr. 15, 52074 Aachen, Germany, e-mail: rolf.wester@ilt.fraunhofer.de
Axel Bäuerle: Fraunhofer Institute for Laser Technology ILT, Steinbachstr. 15, 52074 Aachen, Germany

1 Introduction: optics as an innovation driver in lighting

With the advent of electrical lighting, the light flux emitted by a single light source became bright enough that at times it might not be desirable to have that light source illuminate its surroundings directly. Instead, various items were placed around that light bulb, from simple shields that reduced direct glare to reflectors that could partly redirect the light.

Fast-forward over 100 years, and the transition to LED lighting and advances in ultra-precision machining have created another novelty: freeform optics mass produced from plastics can be positioned close to the compact LED chips due to their low surface temperature. Whereas traditional reflector designs were often limited in their shape to (faceted) parabolic or spherical shapes, the newly available degrees of freedom have led to a revival of a sub-field of optical sciences, optics for illumination, which is now characterized by sophistication and high precision.

Typical conventional optical surfaces are spheres, cylinders, conics or derivatives thereof, whose surface profile can be described by a few parameters. With the evolution of high-precision machining, the number of parameters has increased substantially: for ultra-high resolution applications use of more than 10^5 parameters has been reported. New design paradigms need to be developed that can manage this vast number of parameters. To this end, several algorithms were published, and the aim of this paper is to provide a brief overview of these results.

The aim of Section 2 is to develop categories for the optical design algorithms that have been published so far. Most algorithms published to date need a zero-étendue point source as the light source, and an overview of these is provided in Section 3. Going further towards real-life illumination scenarios, the assumption of a perfectly small source needs to be abandoned in favor of extended sources, which are the topic of Section 4. In Section 5, we present two examples that demonstrate the abilities of freeform optics with regard to complex illumination tasks. Finally, in Section 6 a short summary is given as well as a short discussion concerning problems in the field of nonimaging optical design that need further investigation.

2 Light shaping for illumination follows different approaches

2.1 Imaging versus nonimaging

When optical design is mentioned, this often relates to an imaging setup. Imaging optics aims at bringing all rays emanating from a point on the object as exactly as

possible to the corresponding point on the image plane. The applications of imaging optics cover a wide range, examples include eye glasses, microscopy, astronomy, lithography and photography. The quality of an optical design in imaging optics is often measured by a spot size on the image plane, cf. Figure 1.

Nonimaging optics, by contrast, treat the incoming light as a power source and the main target for the optical designer is to ensure that a prescribed power density is met on a target area. Contrary to the case of imaging optics, no specific importance is placed on the origin of the light ray. The target distribution could be a homogeneous irradiance on a wall in an architectural application, or a complex pattern in the far field, such as for automotive headlamps. Miñano and Benítez [1] provide a definition of imaging and nonimaging optics, respectively, in terms of phase space.

Imaging as well as nonimaging optics are mostly treated within the frame of geometric optics, that is, wave-like effects such as diffraction and interference are neglected. Although a significant number of setups can be correctly modeled geometrically, there are tasks that need correct wave optics treatment. For example, the concept of an image point no longer holds in wave optics. The smallest possible spot size on the image plane is limited by diffraction and given by the Airy disk diameter [2]. Interference fringes can occur depending on the degree of coherence of the radiation at hand. In most applications of imaging and nonimaging optics, incoherent light sources are used, but light sources are never totally incoherent. The important characteristic to quantify these effects is the coherence length, which should be significantly smaller than the expected difference in optical path length between rays.

2.2 Point source versus extended source

The topic of algorithmically designed optics for illumination has seen a major increase in public interest through the increased use of LED technology. Because of their compact size and comparatively low temperature while in operation, LEDs allow for low-cost polymer optics to be placed immediately in front of the light source, often partly enclosing it. In general, the light rays hitting the optical surface at a given point cover a finite range of ray directions $\Delta\vec{s}$ (cf. Figure 2). In the limit of vanishing $\Delta\vec{s}$ the light source can be treated as a point source. The value of $\Delta\vec{s}$ depends on the LED's extend the optics encapsulating the LED and on the distance between source and surface point. In the case of a large divergence angle of the light emanating from the LED, a large distance implies a large size of the optical element. In this case, the 'five times' rule of thumb applies, which means that in the case that the optical surface is five times larger than the source, the point source assumption is approximately valid.

A point source has the advantage that the resulting light distribution has a vanishing phase space volume

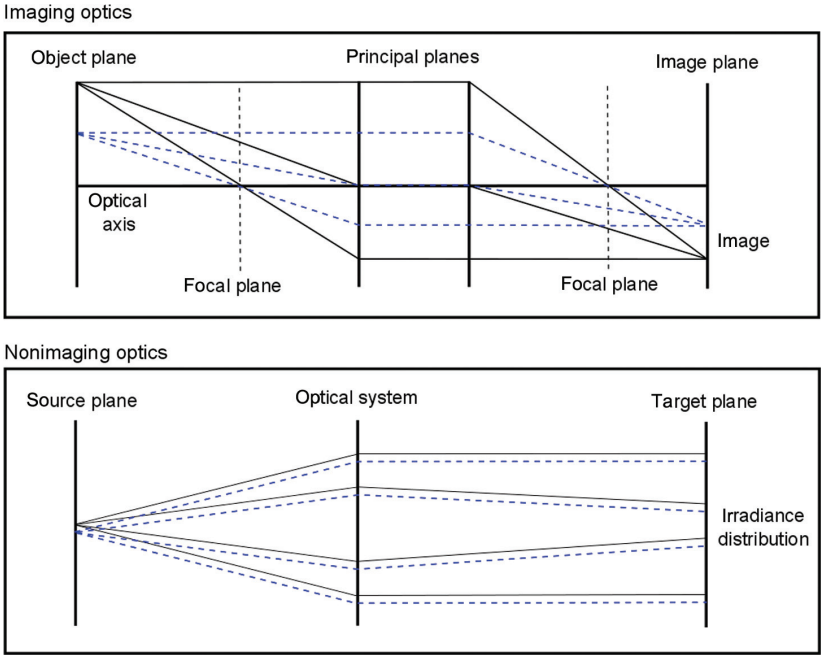

Figure 1 Imaging optics and nonimaging optics setup.

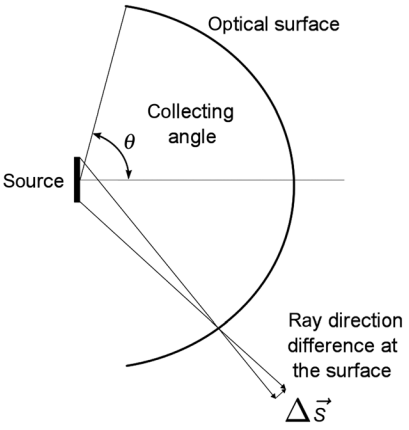

Figure 2 Schema of the setup of light source and optical surface.

(also called a zero-étendue source) and the angle of incidence of light rays for a given point on the optical surface is thus unique. This property allows for the optical design problem to be mathematically well defined, in the sense that under certain restrictive conditions the number of possible solutions can be limited to two [3]. These two solutions differ by the number of caustic points between the optics and the target surface [4]. To the best of the authors' knowledge, no further-reaching formal proof has yet been published that covers the question of existence and uniqueness of a solution [5].

2.3 Number and shape of surfaces

Plane surfaces, that is, surfaces with constant normal vectors, are occasionally used in optics but more interesting surfaces have varying normal vectors. Historically, spherical surfaces dominated optics for several reasons, the main one being the relative simplicity of manufacturing. Cylindrical surfaces are also easy to produce. The corresponding theory of rotationally invariant imaging systems is well developed, which is mainly due to symmetry and the fact that in the so-called paraxial approximation ($\sin\phi \approx \phi$), spherical surfaces allow for simplified calculations.

With the current availability of powerful computers, such approximations are no longer necessary and a typical design procedure uses ray tracing software to optimize surface parameters by setting up a merit function. Therefore, extensions of spherical surfaces, such as conics and aspheres of varying degrees, are used extensively. In the area of nonimaging optics, so-called freeform surfaces have recently found widespread use, fueled by newly developed manufacturing techniques [6]. These surfaces are parametrized by a comparatively high number of parameters, typically 10^2–10^6. Besides regular point clouds, NURBS surfaces on rectangular domains [7] and triangulated surfaces [8] have been used to mathematically describe such surfaces.

An additional criterion to categorize optical design algorithms is by the number of surfaces that are designed. The considerations of existence and uniqueness laid out in the previous section aim at a single optical surface (reflecting or refracting). In many applications, it is desirable to use more than one surface. For example, a lens always has two surfaces, and a choice about the shape of the other surface has to be made in any case. In many cases, it is possible to make a simplifying assumption for the source-facing surface of a lens. For collimated light, a plane surface has no net optical function, and similarly for a point source, a spherical surface shape with its center of curvature at the point source does not refract rays either.

Still, in many cases it is desirable to leverage the additional degrees of freedom obtained through the additional optical surface. For example, the so-called Fresnel reflections at optical interfaces scale in a highly nonlinear way with the angle of incidence [2] (cf. Figure 3B). Figure 3A shows this effect for the interface between glass (n=1.5) and air (n=1.0). If a particularly high angle of deflection is desired, it can be significantly more efficient if two deflections by approximately half the original angle are performed.

Because of the significantly increased number of parameters in comparison with imaging optics, new computational methods are needed to determine the exact shape of freeform optics. These are the subject of Section 3.

2.4 Integrability condition for smooth surfaces

In most practical cases, it is desirable that optical surfaces are smooth or at least smooth within a small number of distinct regions (segments). In general, optical freeform surfaces that generate a prescribed irradiance pattern form a family of surfaces from which a single one has to be picked, for example, by prescribing a spatial position.

A family of smooth surfaces can be described by the level sets of a scalar function $\psi(\vec{r})$. The function value is by definition constant along any tangent to the surface so that the gradient is perpendicular to the surfaces and thus is colinear to the surface normals:

$$\vec{\nabla}\psi(\vec{r}) = |\vec{\nabla}\psi(\vec{r})|\,\vec{N}. \tag{1}$$

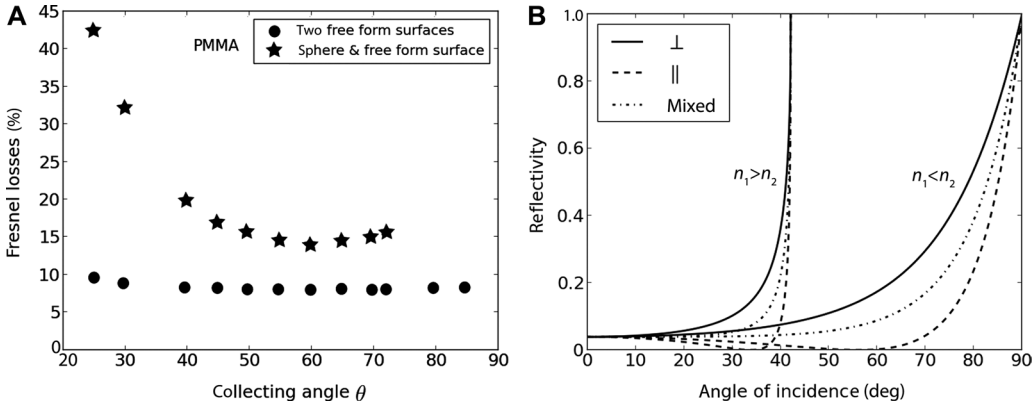

Figure 3 (A) Losses of a PMMA lens for a street lighting application due to Fresnel reflections at both surfaces. The discs designate the case that both surfaces are designed to participate in the ray deflection, whereas the stars designate the case in which the first surface is a sphere with origin at the point source, which means the rays are not deflected by this surface. For an explanation of the collecting angle, see Figure 2. (B) Reflectivity at an interface with refractive indices n_1 and n_2, respectively, as a function of angle of incidence for perpendicular, parallel and mixed polarization.

With $\vec{\nabla}\times(\vec{\nabla}\psi(\vec{r}))=0$ this becomes

$$\vec{\nabla}\times(|\vec{\nabla}\psi(\vec{r})|\vec{N})=\vec{\nabla}(|\vec{\nabla}\psi(\vec{r})|)\times\vec{N}+|\vec{\nabla}\psi(\vec{r})|\vec{\nabla}\times\vec{N}=0. \quad (2)$$

Scalar multiplication with $\vec{N}$ yields

$$(\vec{\nabla}(|\vec{\nabla}\psi(\vec{r})|)\times\vec{N})\cdot\vec{N}+|\vec{\nabla}\psi(\vec{r})|\vec{N}\cdot\vec{\nabla}\times\vec{N}=0, \quad (3)$$

and finally

$$\vec{N}\cdot\vec{\nabla}\times\vec{N}=0. \quad (4)$$

This is the integrability condition that the field of normal vectors has to comply with in order to yield a smooth optical surface. This is a generalization of the integrability condition given in [9]. In coordinates (X, Y, Z), this reads:

$$N_1\left(\frac{\partial N_3}{\partial Y}-\frac{\partial N_2}{\partial Z}\right)=0. \quad (5)$$

$$N_2\left(\frac{\partial N_1}{\partial Z}-\frac{\partial N_3}{\partial X}\right)=0. \quad (6)$$

$$N_3\left(\frac{\partial N_2}{\partial X}-\frac{\partial N_1}{\partial Y}\right)=0. \quad (7)$$

Transforming the coordinate system such that at a given point, the surface normal is given by (0, 0, 1) yields at that point:

$$\frac{\partial N_2}{\partial X}-\frac{\partial N_1}{\partial Y}. \quad (8)$$

The surface can be described locally by a height function $h(X, Y)$. The normal vector is then given by:

$$\vec{N}=\frac{\left(-\frac{\partial h}{\partial X},-\frac{\partial h}{\partial Y},1\right)}{\left|\left(-\frac{\partial h}{\partial X},-\frac{\partial h}{\partial Y},1\right)\right|}=\left(-\frac{\partial h}{\partial X}N_3,-\frac{\partial h}{\partial Y}N_3,N_3\right). \quad (9)$$

Inserting into Eqn (7) and keeping in mind that at the given point $\partial h/\partial X=0$ and $\partial h/\partial Y=0$ this yields the Schwarz integrability condition:

$$\frac{\partial^2 h}{\partial Y\partial X}-\frac{\partial^2 h}{\partial X\partial Y}=0. \quad (10)$$

3 Irradiance tailoring for point sources

Most optical freeform surface design algorithms rely on the point source assumption. An exception is the simultaneous multiple surface (SMS) method, an extension of the method of Cartesian ovals, developed by Miñano and others [10–12] that allows to construct a two-surface system that exactly maps two input congruences to two output congruences (a congruence is a zero-étendue light field). By construction, it is two-dimensional (one transverse dimension). This method has been applied to imaging as well as nonimaging optical problems and has been extended to handle three-dimensional systems at least approximately [12].

3.1 Irradiance tailoring as the Monge-Kantorovich transport problem

Mathematically, the problem of finding a ray path from the source plane to points on the target plane can be described as coordinate mappings:

$$x_t = x_t(x_s, y_s) \tag{11}$$

$$y_t = y_t(x_s, y_s). \tag{12}$$

The index t designates target coordinates and the index s source coordinates, respectively. The requirement of total radiation power conservation leads to:

$$\int_S E_s(x_s, y_s)\,dx_s dy_s = \int_T E_t(x_t, y_t)\,dx_t dy_t. \tag{13}$$

Transforming the integral on the right-hand side to source coordinates yields:

$$\int_S E_s(x_s, y_s)\,dx_s dy_s = \int_S E_t(x_t(x_s,y_s), y_t(x_s,y_s)) \left|\det(J(x_s,y_s))\right| dx_s dy_s, \tag{14}$$

with the Jacobian matrix of the mapping:

$$J = \begin{pmatrix} \frac{\partial x_t}{\partial x_s} & \frac{\partial x_t}{\partial y_s} \\ \frac{\partial y_t}{\partial x_s} & \frac{\partial y_t}{\partial y_s} \end{pmatrix}. \tag{15}$$

We require the mapping to be smooth and one-to-one so that the point-wise relation results as follows:

$$E_s(x_s, y_s) = E_t(x_t(x_s, y_s), y_t(x_s, y_s))|\det(J(x_s, y_s))|. \tag{16}$$

There is no unique mapping that complies with Eqn (16). Further requirements have to be set up, one important one is that the mapping can be realized by a smooth optical surface. Eqn (16) together with further conditions leads to a Monge-Ampère type equation.

3.2 Solution methods

A direct solution of Monge-Ampère type equations is fairly demanding mathematically. Schruben [13] derived an equation that describes the mapping of a reflector problem but did not provide a solution. Solution methods have been developed for special setups but are still not applicable to real-world optics design problems.

3.2.1 High-resolution tailoring using surface curvatures

Ries and Muschaweck [14] describe a method that computes a Monge-Ampère type equation indirectly. A given optical surface generates an irradiance distribution $E_g(\vec{t})$ on the target as a function of the target coordinates $\vec{t}$. If the desired irradiance distribution is given by $E_p(\vec{t})$ the difference:

$$\Delta E(\vec{t}) = E_g(\vec{t}) - E_p(\vec{t}) \tag{17}$$

has to vanish. The irradiance generated by the optical surface on the target plane is computed using the curvature tensors of the optical surface and the input ray bundle, respectively, and Snell's law of refraction. The surface is parametrized smoothly so that the solution complies with the integrability condition. The parameters describing the surface are determined such that Eqn (17) vanishes everywhere on the target. Although Eqn (17) is not a Monge-Ampère type equation, the solution complies with Eqn (16).

3.2.2 High-resolution tailoring using flux prisms

Bruneton et al. [15] describe a variant of this approach. Instead of using the irradiance, which can diverge if there are caustics, they use radiant power differences and minimize the difference between generated and prescribed radiant powers. If the number of independent parameters equals the number of equations, least-squares minimization and root finding as in [14] are mathematically equivalent. The radiant powers are calculated using area elements of the ray bundles on a surface near the source and the target surface, respectively.

Monge-Ampère type equations as well as the equations resulting from the Ries or Bruneton treatment of the problem are highly nonlinear, and thus solutions can in general only be found by iterative methods with initial values sufficiently close to the final solution. Good initial values can be found either by some other method or by a multi-grid method that starts with a coarse grid and iteratively refines the resolution.

3.2.3 Method of ellipsoids and paraboloids

In a series of papers, Oliker and coauthors [16–19] published the method of ellipsoids and paraboloids, respectively. The key idea is to place the point source at the location of one of the paraboloid/ellipsoid foci and the

other on the target plane. There are a prescribed number of overlapping paraboloids/ellipsoids. The radiant power on the target caused by a given paraboloid/ellipsoid is given by the radiant power from the source that hits the active surface area of the paraboloid/ellipsoid. A major problem with this method is the calculation of the active surfaces of the paraboloids/ellipsoids. Besides this, the resulting surfaces are patches of paraboloids/ellipsoids that in general do not exhibit smooth transitions.

3.3 Two step methods

As pointed out above, a ray mapping has to generate the desired irradiance distribution and simultaneously has to comply with the integrability condition Eqn (4). The combination of both requirements leads to highly nonlinear equations that are difficult to solve. From a numerical point of view, it would be much easier to separate the procedure into two steps:

1. Find a ray mapping that creates the desired irradiance.
2. Reconstruct the surface from the normal vector field that can be derived from the ray mapping.

The problem with this approach is not how to find a ray mapping that creates the desired irradiance but to meet the integrability condition at least approximately.

3.3.1 Finding a suitable ray mapping

The simplest ray mapping can be found by two consecutive 1-d mappings [20] but the results are rather poor in terms of integrability of the resulting surface. In literature, ray mappings are described that are improvements compared to this simplistic approach. Parkyn [9] found a ray mapping by 'a one-to-one correspondence between constant-flux source-grid cells on the sphere of directions from the source and the uniformly sized rectangular cells of a target grid'. Wang et al. [21] perform a light energy mapping between the light source and target. Bäuerle et al. [22] solved a Monge-Ampère equation subject to minimizing a generalized Monge-Kantorovich functional.

3.3.1.1 Ray mapping as a solution of a Monge-Kantorovich problem

A unique mapping that complies with Eqn (16) can be found by requiring that the generalized Monge-Kantorovich functional is minimized by the map:

$$M(u)=\int F(x_s, y_s, x_t(x_s,y_s), y_t(x_s,y_s))E_s(x_s,y_s)dx_s dy_s. \quad (18)$$

For the L^2 cost function $F(x_s, y_s, x_t, y_t)=(x_s-x_t)^2+(y_s-y_t)^2$, it has been shown that the coordinate mapping is irrotational and is given by the gradient of a convex function u [23]:

$$x_t=\frac{\partial u(x_s, y_s)}{\partial x_s}, \quad (19)$$

$$y_t=\frac{\partial u(x_s, y_s)}{\partial y_s}. \quad (20)$$

With this, we get a Monge-Ampère type equation:

$$E_s(x_s,y_s)=E_t\left(\frac{\partial u(x_s, y_s)}{\partial x_s}, \frac{\partial u(x_s, y_s)}{\partial x_s}\right) \left(\frac{\partial^2 u}{\partial x_s^2}\frac{\partial^2 u}{\partial y_s^2}-\frac{\partial^2 u}{\partial x_s \partial y_s}\frac{\partial^2 u}{\partial y_s \partial x_s}\right). \quad (21)$$

Although this is a solution of the formal mapping problem Eqn (14), this mapping is unlikely to comply with the integrability condition Eqn (4) because the above derivation does not include any information about the optical setup or the optical surface. No direct link could yet be established between Eqn (4) and the rotationlessness of the solution of Eqn (21); nevertheless, it seems reasonable that the deviation of the left-hand side of Eqn (4) at least becomes smaller if the mapping is rotation-free. In [15] the improvement is demonstrated.

3.3.1.2 Computing ray mapping by the method of paraboloids

Fournier et al. [24–26] computed the mapping using the Oliker method with a small number of paraboloids and the resulting function is fitted to a finer grid. With this mapping given, a surface is reconstructed. This approach avoids the paraboloid method problem of nondifferentiable surfaces.

3.3.2 Reconstructing the optical surface from a mapping

With the mapping information, the optical surfaces can be computed so that the source rays are deflected to hit the target at the desired positions. Surface reconstruction from normal vectors is a known problem, for example, in the field of reverse engineering. Many different methods have been developed for this task. Nam and Rubinstein [27] and Rubinstein and Wolansky [28] discuss the issue

in detail. Because the ray mappings discussed in the previous section in general do not exactly comply with the integrability condition, a reconstruction method based on a least-squares optimization method seems most suitable.

We suppose the surface to be parametrized by:

$$\vec{r}(i)=\vec{r}_0(i)+\lambda(i)\vec{s}(i), \tag{22}$$

with $\vec{r}_0(i)$ the origin of ray i. This can be the position of a point source or the position of the ray after passing through another optical surface. $\vec{s}(i)$ is the unit direction vector of the ray and $\lambda(i)$ is a scalar parameter defining the surface point i. The point $\vec{r}(i)$ can be a surface point of a regular Cartesian grid, a node of a triangulated surface or a control point of a NURBS surface. $\vec{s}(i)$ and the surface normal vector $\vec{N}(i)$ give the direction vector $\vec{s}_o(i)$ of the ray after refraction (or reflection) at the surface. Given $\vec{s}_o(i)$ and the ray's position on the optical surface $\vec{r}(i)$, the point $\vec{T}(i)$ where the ray intersects the target surface can be computed. Assuming that the target positions $t_x^{(i)}(\lambda)$ and $t_y^{(i)}(\lambda)$ of the rays as computed by the mapping can be realized by a smooth, integrable surface the objective function to minimize is given by:

$$F(\lambda)=\sum_i\left[\left(T_x^{(i)}(\lambda)-t_x^{(i)}(\lambda)\right)^2+\left(T_y^{(i)}(\lambda)-t_y^{(i)}(\lambda)\right)^2\right] \tag{23}$$

where $T_x^{(i)}(\lambda)$ and $T_y^{(i)}(\lambda)$ are the actual local target coordinates of the ray for a given vector of parameters λ. Because the normal vector field deduced from the ray mapping need not be integrable, the mapping realized by the surface in general deviates from the computed ray mapping and as a consequence the irradiance distribution deviates from the prescribed distribution too. The amount of irradiance distribution deviation is hardly known in advance so that the quality of the result has to be examined for every setup. Although currently there is no hard mathematical proof, it is plausible to assume that the smaller the violation of the normal field integrability condition, the smaller will be the irradiance distribution deviation. The relationship between the rotation of the mapping and the value of Eqn (4) has been examined in [29].

Besides computational efficiency a further advantage of the two step approach is that the total light deflection can easily be split into several parts, each one realized by a separate optical surface [22, 30].

NURBS surfaces are widely used in computer graphics and CAD systems but using triangulated surfaces has the advantage of being very flexible for further processing of the resulting surfaces. They can, for example, be refined or cut very quickly, thus gaining finer control over the resulting lens's boundary conditions. In combination with a multi-surface design, this also allows to include manufacturing constraints (e.g., to avoid undercuts for injection molding).

4 The challenge of irradiance tailoring for extended sources

Thus far, only point sources have been considered. But real light sources are extended. As long as the optical element is large compared to the light source, the point source assumption is a good approximation. The demands of higher light fluxes, realizable by light modules with diameters in the range of several 10–100 mm, and small lamp sizes make it necessary to consider the source extension more thoroughly.

With zero-étendue point sources (almost) any irradiance distribution can be realized. This no longer holds for extended sources. The limit is given by the étendue of the light bundles which cannot take on smaller values at the target plane than it had at the source.

Because at present no optical freeform design method can manage extended sources directly (the SMS method can at best treat two or three normal congruences, e.g., point sources), point source algorithms have been modified or extended to tackle the issue of extended sources.

4.1 Optimization of parameters

Fournier et al. [31] used a point source algorithm wrapped by an additional optimization loop in which the location of a point source is varied such that the irradiance distribution realized by an extended source located at a fixed point is close to the desired distribution.

4.2 Adaptation of the point source target distribution

A different approach was published by Bortz and Shatz [32] where the prescribed target distribution that is used with a point source algorithm is adapted so that the desired distribution is realized by the calculated surface when applying an extended source (Figure 4). Bortz and Shatz use the following iterative adaptation rule:

$$I_p^{(n+1)}(x)=c\,\frac{I_p^{(n)}(x)}{I_t^{(n)}(x)}I_r(x) \tag{24}$$

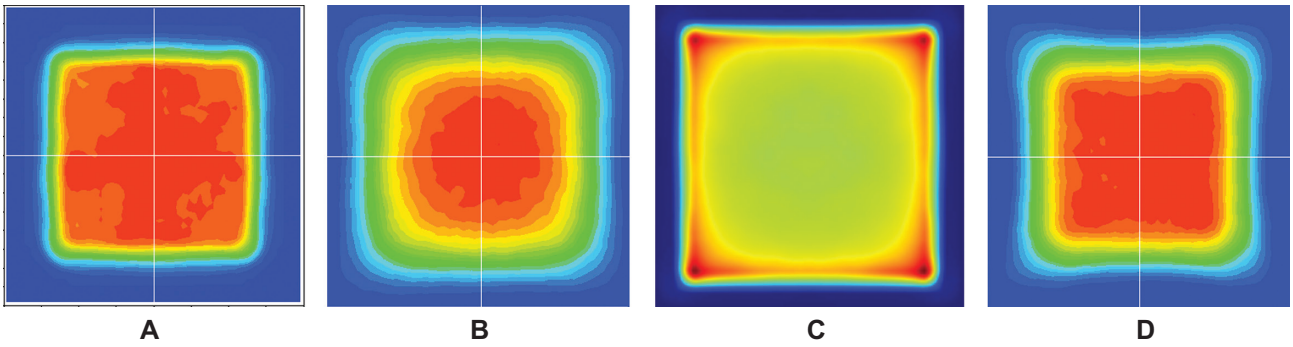

Figure 4 (A) Target distribution produced by a point source, (B) corresponding target distribution due to an extended source, (C) new prescribed distribution, (D) resulting extended source distribution after one iteration step.

$$I_p^{(0)}(x) = I_r(x) \tag{25}$$

$I_r(x)$ is the required output distribution, I_t^n the ray-traced output distribution at step number n and $I_p^{(n+1)}$ the prescribed distribution that is used in step number n+1. c is a normalization factor to ensure total power conservation.

Bruneton et al. [15] modified this approach by employing solutions of the Monge-Kantorovich problem as discussed in Section 3.3.1. Figure 4A shows the target distribution computed by ray tracing the rays of a point source through a lens designed using a point source algorithm. Figure 4B shows the target distribution in the case of an extended source. The method described in Section 3.3.1 is used to compute the mapping function that transforms the distribution Figure 4B into the distribution Figure 2B. This mapping function is then applied to the distribution Figure 4A resulting in Figure 4C, which is used as the prescribed distribution in the next iteration. Figure 4D shows the distribution of an extended source traced through the lens computed with a point source algorithm using the prescribed distribution itadapc. Further iterations did not improve the result.

5 Sample applications of nonimaging optics

Freeform nonimaging optics have enabled a series of technological innovations in the domain of light shaping for illumination. Examples that have now found widespread use are LED street lighting, architectural lighting and automotive lighting. Whereas all these applications only fulfill a single optical function and aim to achieve relatively low-resolution irradiance patterns, the following two sections will outline some of the new advances in this field.

5.1 Integrating extended functionality: automotive lighting

Currently, nonimaging automotive lighting units only fulfill signaling functions, that is, the light from this unit is meant to be received directly by an observer. Examples include turn indicators, braking lights or daytime running lights. Going further from there, actual

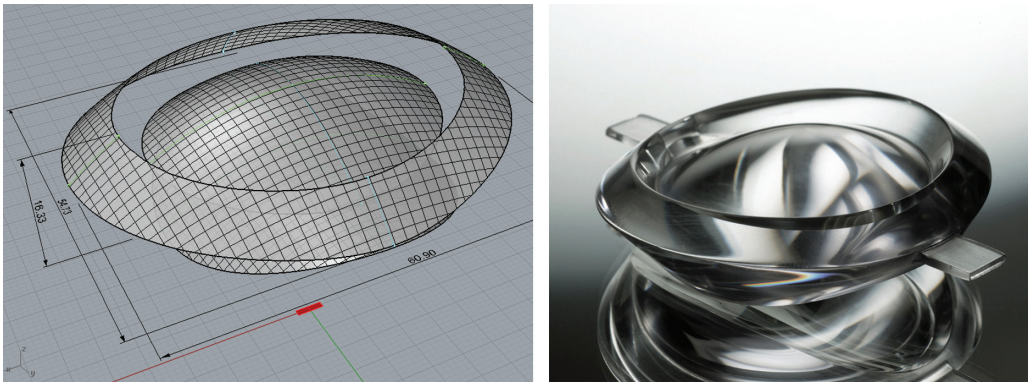

Figure 5 Rendering and photo of an automotive fog light lens for use with an LED light source. Dimensions are in mm.

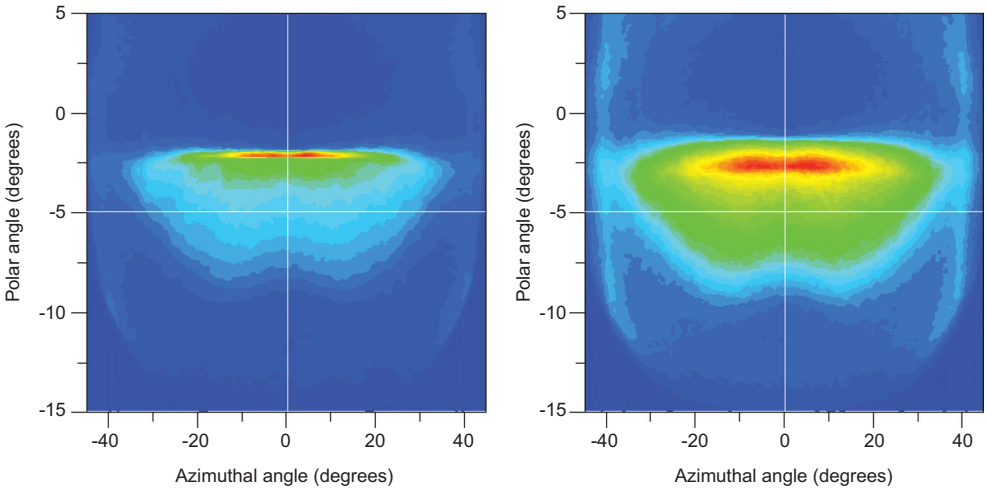

Figure 6 Angular light distribution achieved by a point source (left) and by a 4×1 mm² automotive LED (right) in combination with the lens designed using the point source assumption from Figure 5.

illumination applications can be targeted, where the information relevant to the viewer does not come from looking at the light source itself but from the object that is illuminated. One challenge here in automotive applications is the need to reduce glare for oncoming traffic. This is realized through a steep bright-dark cut-off at the horizon. Figure 5 shows a rendering and a photo of a monolithic lens for an LED lighting module. Looking at the light distribution in Figure 6, which is created by this lens in combination with a 4×1 mm² automotive LED, the bright-dark cut-off becomes immediately apparent. A more thorough analysis yields that the resulting distribution indeed conforms to current industry practices and regulations [15].

To achieve this, the two optical surfaces for the fog light function are designed using Bruneton's mapping optimization algorithm from Section 3.3.1. To this end, a first ray mapping is found by successively integrating along the Cartesian coordinate axes, and then this mapping is optimized to make it rotation-free. Finally, the optical surfaces are reconstructed using an optimization for a triangulated surface.

5.2 High-resolution tailoring: logo lens

The main technological challenge in the previous example of a fog light lens is to achieve a sufficiently strong bright-to-dark cut-off at the horizon. Apart from this, the desired distribution shows rather low variation and feature resolution. This section, by contrast, will demonstrate the power of algorithmically designed nonimaging optics with another example. Figure 7 shows the rendering of a lens together with the rather complicated irradiance pattern it generates (a logo) [33]. The resolution of the prescribed target distribution is 193×193 pixels, and the contrast is approximately 4:1. Even though higher contrasts can be realized, the minimum irradiance is limited by the

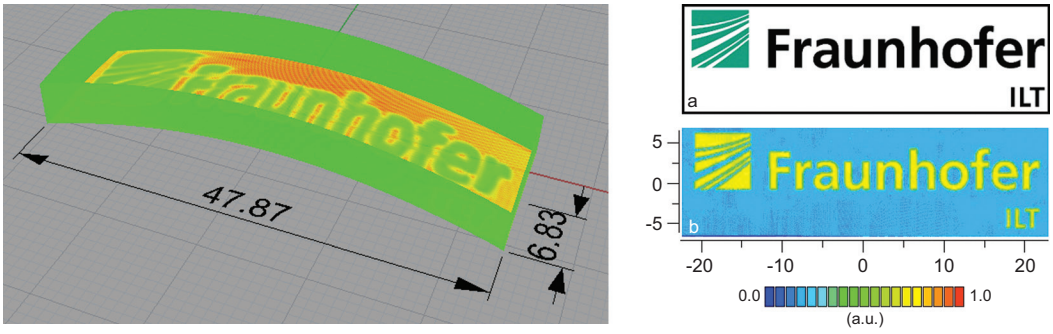

Figure 7 (Left) Rendering and false color representation of surface curvature of a freeform lens that creates a logo distribution. All dimensions are in mm. (Right) Target and actual irradiance pattern as found in ray tracing analyses.

maximum optical surface curvature of smooth surfaces that can be manufactured.

This lens was designed using the flux-prism method proposed by Bruneton et al. (cf. Section 3.2.2). Calculation times are a few minutes on a standard computer.

6 Conclusion

In this paper, an overview of current light shaping methods for illumination is given. To this end, the different categories of optical design are explained. Focusing on algorithms for the design of nonimaging optics for point sources, a review of published design methods is given. To conclude, two examples showcasing the possibilities of nonimaging optics are given.

Two main problems in light shaping for lighting still persist: extended sources and color effects. From a theoretical point of view, a phase space description is the adequate framework for treating finite étendue sources, whereas from a numerical point of view it would be advantageous to stay with the spatial description. Further investigations are necessary to find a suitable solution that accounts for the finiteness of real light sources but which stays acceptably efficient.

Light quality not only depends on radiance and its distribution but also on color. The relevant keywords here are color temperature, color rendering index (CRI) and color homogeneity. In the field of lighting, continuous spectra that resemble the spectrum of sun light are almost always desired. LEDs emit light within relatively small wavelength regions of <10 nm. To obtain color perception, at least comparable with that of sun light, the light emitted by blue LEDs is typically transformed into white light through the use of fluorescent materials. This can be combined with LEDs emitting in the blue, green and red region of the spectrum, respectively. A major problem with white LEDs is that due to their design, the emitted light spectrum varies with the direction of emission. This effect is called 'color over angle effect'.

Likewise, dispersion is a common problem in optics. In imaging optics, chromatic aberrations can be reduced by using combinations of lenses with different glass materials or by combining refractive and diffractive optical elements [34]. This is normally not an option for lighting applications due to cost considerations. In the field of lighting, reflectors can alternatively be employed which do not show dispersion (besides wavelength-dependent reflectivity). LED arrays with LEDs emitting at different wavelengths need to be equipped with light mixing elements such as Kohler lens arrays [35].

Acknowledgments: This work has partly been funded by the German Federal Ministry of Education and Research (BMBF) within its program on freeform optics (grant numbers 13N10832, 13N10833).

Received May 24, 2013; accepted July 4, 2013

References

[1] J. C. Miñano and P. Benítez, Proc. SPIE 3781, 2–11 (1999).
[2] M. Born and E. Wolf, in 'Principles of Optics: Electromagnetic Theory of Propagation, Interference and Diffraction of Light' (Cambridge University Press, Cambridge, 1999), 440–442.
[3] R. Courant and D. Hilbert, in 'Methoden der Mathematischen Physik II', 2nd ed., Vol. Band 31, Heidelberger Taschenbücher (Springer, Heidelberg, 1968), p. 277.
[4] L. Marder, Proc. R. Soc. Lond. A Math. Phys. Sci. 378, 529–538 (1981).
[5] S. A. Kochengin and V. I. Oliker, Inverse Probl. 13, 363–373 (1997).
[6] S. Bäumer, Ed., in 'Handbook of Plastic Optics', 2nd ed. (Wiley-VCH, Weinheim, 2010), 35–66.
[7] L. Piegl and W. Tiller, in 'The NURBS Book' (Springer, Berlin/Heidelberg, 1997), p. 100.
[8] M. S. Floater, in 'Computer Aided Geometric Design', 14.3, 231–250 (1997).
[9] W. A. Parkyn, Proc. SPIE 3428, 154–162 (1998).
[10] J. Miñano, P. Benítez, W. Lin, F. Muñoz, J. Infante, et al., Proc. SPIE 7429, 74290C-1–74290C-8 (2009).
[11] J. C. Miñano, P. Benítez and A. Santamaría, Opt. Rev. 16.2, 99–102 (2009).
[12] P. Benítez, J.-C. Miñano, J. Blen, R. Mohedano, J. Chaves, et al., Opt. Eng. 43.7, 1489–1502 (2004).
[13] J. S. Schruben, J. Opt. Soc. Am. 62.12, 1498–1501 (1972).
[14] H. Ries and J. Muschaweck, J. Opt. Soc. Am. A 19.3, 590–595 (2002).
[15] A. Bruneton, A. Bäuerle, M. Traub, R. Wester and P. Loosen, Proc. SPIE 8485, 84850H (2012).
[16] V. I. Oliker, Inverse Probl. 5, 51–65 (1989).
[17] S. Kochengin, V. Oliker and O. von Tempski, Inverse Probl. 14, 661–678 (1998).
[18] L. A. Caffarelli, S. A. Kochengin and V. I. Oliker, Contemp. Math. 226, 13–32 (1999).
[19] V. Oliker, Proc. SPIE Int. Opt. Des. Conf. 6342, 634211-1–634211-12 (2006).
[20] L. Wang, K. Qian and Y. Luo, Appl. Opt. 46.18, 3716–3723 (2007).
[21] K. Wang, S. Liu, F. Chen, Z. Qin, Z. Liu, et al., J. Opt. A Pure Appl. Opt. 11, 105501 (2009).

[22] A. Bäuerle, A. Bruneton, R. Wester, J. Stollenwerk and P. Loosen, Opt. Express 20.13, 14477–14485 (2012).
[23] R.-J. M. W. Gangbo, Acta Math. 177, 113–161 (1996).
[24] F. R. Fournier, W. J. Cassarly and J. P. Rolland, Proc. SPIE 7423, 742302 (2009).
[25] F. R. Fournier, W. J. Cassarly and J. P. Rolland, in 'International Optical Design Conference and Optical Fabrication and Testing' (Optical Society of America, 2010) IWB4.
[26] F. R. Fournier, W. J. Cassarly and J. P. Rolland, Opt. Express 18, 5295–5304 (2010).
[27] J. Nam and J. Rubinstein, J. Opt. Soc. Am. A 25, 1697–1709 (2008).
[28] J. Rubinstein and G. Wolansky, Opt. Rev. 8, 281–283 (2001).
[29] A. Bruneton, A. Bäuerle, R. Wester, J. Stollenwerk and P. Loosen, Opt. Lett. 38.11, 1945–1947 (2013).
[30] B. Parkyn and D. Pelka, Proc. SPIE 6338, 633808-1–633808-7 (2006).
[31] F. R. Fournier, W. J. Cassarly and J. P. Rolland, Proc. SPIE 7103, 710301-1–710301-10 (2008).
[32] J. Bortz and N. Shatz, Proc. SPIE 6670, 66700A (2007).
[33] A. Bruneton, A. Bäuerle, R. Wester, J. Stollenwerk and P. Loosen, Opt. Express 21.9, 10563–10571 (2013).
[34] T. Nakai and H. Ogawa, in 'Diffractive Optics and Micro-Optics' (Optical Society of America, 2002) DMA2.
[35] M. Hernández, A. Cvetkovic, P. Benítez and J. C. Miñano, Proc. SPIE 7059, 705908 (2008).

Rolf Wester is a scientist at the Fraunhofer ILT in Aachen. He received his Diploma (MSc) in Physics in 1983 from the Technical University of Darmstadt and his Doctorate (PhD) in 1987 from the RWTH Aachen. In the same year he changed from the RWTH to the Fraunhofer ILT where he continued working on high frequency excitation of gas lasers. In recent years, his field of research interest switched to optics. He is now mainly concerned with the development of simulation software for physical optics problems and of numerical design tools for freeform optical elements.

Axel Bäuerle received his MSc in Physics in 2008 from Imperial College, London (UK), working on high-power solid lasers. He joined RWTH Aachen University and Fraunhofer ILT in 2009, where he is a scientist working on algorithms to design freeform optical surfaces.